

How to get spatial resolution inside probe volumes of commercial 3D-LDA systems

by

V. Strunck, T. Sodomann, H. Müller, D. Dopheide

Section of Fluid Flow Measuring Techniques, Physikalisch-Technische Bundesanstalt

Bundesallee 100, 38116 Braunschweig, Germany

tele #49-531-592-1311, fax #49-531-592-1305

<mailto:volker.strunck@ptb.de>

1. INTRODUCTION

In Laser Doppler Anemometry (LDA) it is often the aim to determine the velocity profile for a given fluid flow. As other methods common LDA techniques rely on measuring the velocity in a probe volume and then varying its position in the test section. The spatial resolution of such velocity profile is limited in principal by the size of the probe volume. A conventional solution for a better resolution in 3-D LDA systems is to use the coincidence window technique to evaluate only signals of at least two velocity components that appear in a given time interval and thus decrease virtually the size of the probe.

Our new and easy method shown below allows improvements of the spatial resolution by at least one order of magnitude and measurements of small scale velocity profiles inside the measuring volume of a commercial available 3D-LDA while leaving the measuring apparatus fixed. No change of the optical set-up is necessary. Instead of discarding valuable signal data outside a coincidence window all velocity signals are recorded with a multi-channel storage oscilloscope and fed into a computer. The determined difference of arrival times of a signal pair is equal to the time of flight of a scattering particle between both measuring volumes used and is a function of its passage due to the geometry.

2. THEORY

In standard 3-D (backscatter) LDAs one optical component (514 nm) often measures the main stream velocity u , a second (488 nm) the vertical velocity w . The third component (476 nm) measures in combination with the first component the transverse velocity v using an off-axis arrangement. The measuring volume for the main stream and the transverse velocity lie in a plane as illustrated in figure 1.

A scattering particle passing both measuring volumes generates two signals that are more or less coincident depending on its passage and the separation of the measuring volumes due to their geometry. Depending on their passage through the two measuring volumes the signals of the scattering particles in the channels of the 488 nm and 476 nm component differ in frequency as well as in arrival times. For path 1 the 476 nm component appears firstly, for path 3 the 514 nm component is the first one. Only in the cross point (path 2) both signals are simultaneous. We simply measure the time of flight Δt of a particle between both measuring volumes, and of course, their accompanying velocities [Strunck et al (1993), Strunck et al (1994)].

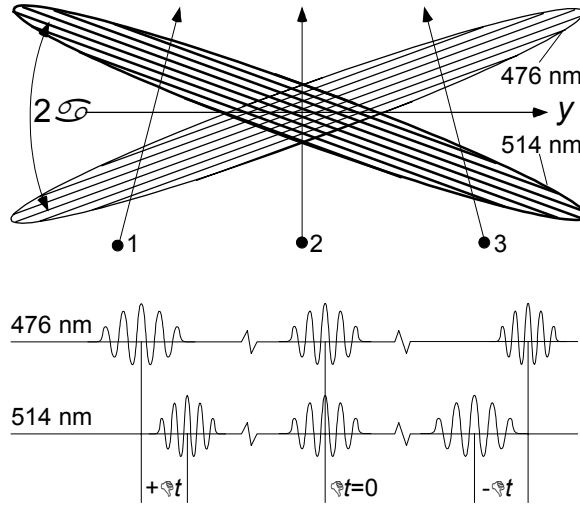


Fig. 1: Two measuring volumes (top view), paths of particles and their signals

Having received the velocity data of the components and the angle between the axes of both measuring volumes, the streamwise velocity u (in x direction) and the transverse velocity v (in y direction) is obtained using

$$u = (u_{514} + u_{476})/2 \cos \alpha, \quad v = (u_{514} - u_{476})/2 \sin \alpha \quad (1)$$

With an angle 2α between the measuring volumes and assuming a flow parallel to the x -direction the distance y of the scattering particle to the cross-over point is

$$y = \frac{u \Delta t}{2 \tan(\alpha)}. \quad (2a)$$

For an inclined flow with an angle of β to the x -direction the transverse velocity is non zero and the distance y to the cross-over point is

$$y = \frac{\cos(\alpha - \beta) \cos(\alpha + \beta)}{\cos \beta \sin 2\alpha} \cdot \sqrt{u^2 + v^2} \cdot \Delta t, \quad \beta = \arctan(v/u) \quad (2b)$$

Unfortunately, modern LDA signal analysers do not precisely record the time stamps of signals. The only option they have is to set a maximum delay time between two signals to reject signals outside of this 'coincidence time' window. To measure delay times, signals have to be recorded by a multi-channel transient recorder and processed separately. The frequency f_D is extracted from the centre of gravity of the peak in the amplitude spectrum of the signal and the time stamp t_S from the gradient of the phase Φ in the phase spectrum at the peak position [Albrecht et al (1993), Borys et al (2000)]:

$$t_s = \frac{1}{2\pi} \frac{d\Phi}{df} \quad (3)$$

t_S is a measure of the appearance of the signal centre in the acquisition time window of the transient recorder. For two synchronously recording channels the time delay between the signals simply is the difference of these time stamps. Knowing the time stamps t_{S1} and t_{S2} of both Doppler signals in the synchronously recorded time windows, the time of flight Δt of a scattering particle is

$$\Delta t = t_{S2} - t_{S1}. \quad (4)$$

To show the dependence of time stamp and phase difference, an artificial LDA-signal is investigated:

$$LDA(t) = (1 + \cos(2\pi f_1 t + \theta)) \cdot \cos(2\pi f_n t + \gamma); \quad \theta = (2\pi/T) \cdot t_s; \quad f_i = i/T; \quad t \in \{0..T\} \quad (5)$$

The first term of the product is the envelope of the filtered signal and Θ defines its position of the maximum in the time window T . The second term is the carrier (LDA-signal frequency f_n) with a frequency n times larger the first harmonic f_1 in the time window. It has to be pointed out that there are n periods in this artificial LDA-signal. γ is an arbitrary phase of the carrier. Rewriting yields

$$LDA(t) = \frac{1}{2} \cdot \cos(2\pi f_{n-1}t + \gamma - \Theta) + \cos(2\pi f_n t + \gamma) + \frac{1}{2} \cdot \cos(2\pi f_{n+1}t + \gamma + \Theta). \quad (6)$$

The central difference (using the side bands of the signal) with respect to frequency gives

$$\left. \frac{d\Phi}{df} \right|_n = \frac{(\gamma + \Theta) - (\gamma - \Theta)}{f_{n+1} - f_{n-1}} = \frac{\Theta}{f_1} = \Theta T = 2\pi \cdot t_s \quad (7)$$

The phase γ of the carrier has no influence on the position of the signal in the time window, because it is simply an offset. Θ is always positive, so 2π ambiguities in the phase gradient due to the cyclic character of the Fast Fourier Transform (FFT) are easily removed by adding 2π if the phase difference becomes negative. The phase gradient is determined using a linear regression and the phases belonging to the frequency distribution of the *Doppler peak*. The algorithm above to determine the position of a signal in the time window is versatile when the FFT is used to estimate the Doppler frequency, because besides the power spectrum then also the phase spectrum is available.

3. SET-UP

The set-up procedure for the 3D-LDA has almost been described in the accompanying manuals. For our purpose it must be guaranteed that the coincidence mode of the system is working well, thus, all beams must have the same cross-over point. But, instead using the acquisition system, we connect a small circuit to the output lines of two photo multipliers, the Bragg cell output and the trigger output of a Dantec BSA F80 (figure 2). The excellent trigger output verifies that LDA signals only start our acquisition system, which has a simple level trigger option. The output signals from the photo multipliers are down mixed to the base band with the Bragg cell frequency. After filtering the signals with a low pass, the shift frequency has been removed and the signals are like those of a not shifted LDA. The LDA signals are then fed to a storage oscilloscope and read by a PC for further reduction.

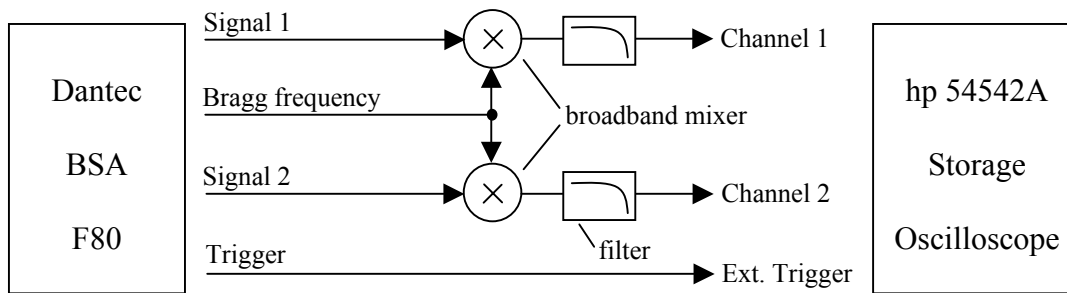


Fig. 2 Electronic set-up with acquisition system

Due to the IEEE-link the scope data rates have been decreased to 40 LDA-signals per second. Also the Bragg cell driver is sensitive to a second link. Broadband mixers operate only with certain voltage levels. All in all, with an signal-to-noise ratio limited to at least 5 dB on both channels, data rates of five validated signals per second could be obtained.

4. VERIFICATION

To obtain the maximum length of the two measuring volume probes we move a wire with a diameter of $5\mu\text{m}$ through the measuring volume (figure 3) of our LDA that has a working distance of 1,60 m.

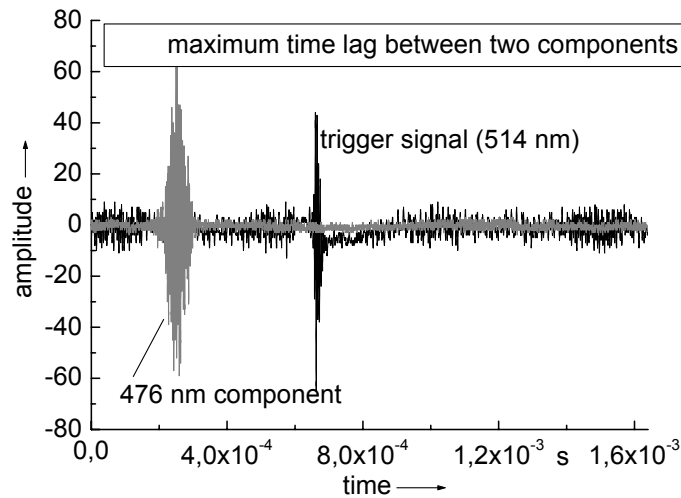


Fig. 3: Signals of a scattering wire moved on path 1 outlined in figure 1

The effective probe length with 4 mm in this case is very long due to the fact of a good plane flow simulation (the wire always hits both measuring volumes). Compared to the theoretical length of the measuring volumes one half can be used. However, in a real flow the particles are small spheres and their flight directions differ from a plane flow.

5. MEASUREMENTS

Two applications will be shown. One is to calibrate and to prove the parallelism of the fringe system and the second is to measure a flow near the stagnation point of a cuboid.

5.1 CALIBRATION

The probe volumes are focussed into the middle of an empty wind tunnel. A plane flow is assumed. The obtained measurement shows that fringe spreading is below 1% (figure 4).

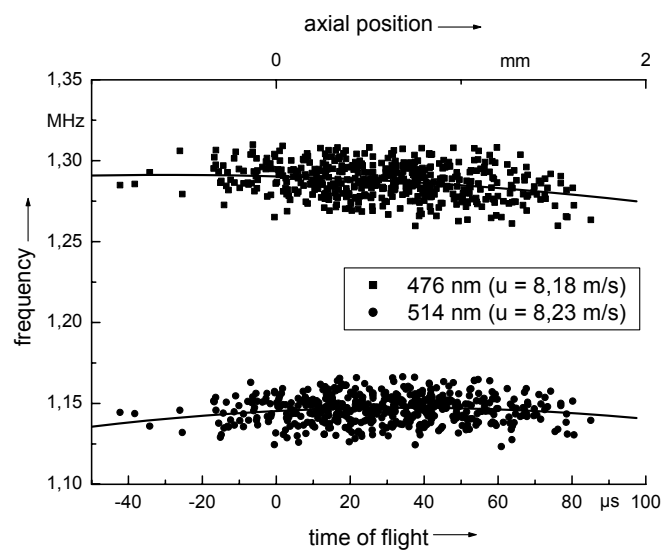


Fig. 4: Spatial resolution of the probe in a plane flow and fringe spreading

The effective probe length has decreased to 2 mm. This is not only an effect of flow but also of the decrease of signal to noise ratio (SNR) due to the larger acquisition time window. New algorithms could be introduced to diminish this problem.

Knowing the fringe spreading along the measuring volumes allows to determine a local fringe distance and also to calculate the offset of artificial turbulence in a selected time window when using the coincidence mode of modern acquisition systems.

5.2 FLOW NEAR THE STAGNATION POINT OF AN OBSTACLE

The following flow situation has been investigated (figure 5):

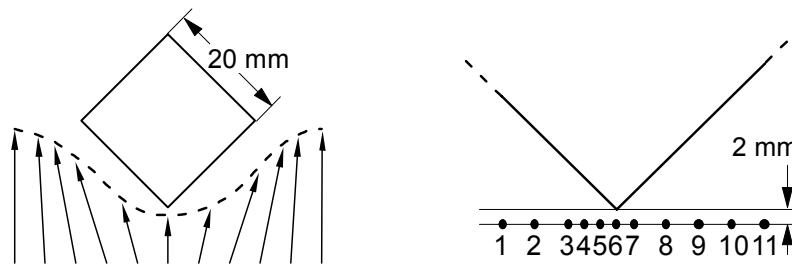


Fig. 5 Sketch of a flow around a cuboid and measuring positions used

To demonstrate the resolution a gradient in a flow is needed. A cuboid has been taken as an obstacle in a wind tunnel. Two millimetres in front of the stagnation point at the corner of the cuboid the main stream velocity decreases from about 10 m/s down to 2,7 m/s (Fig 6a).

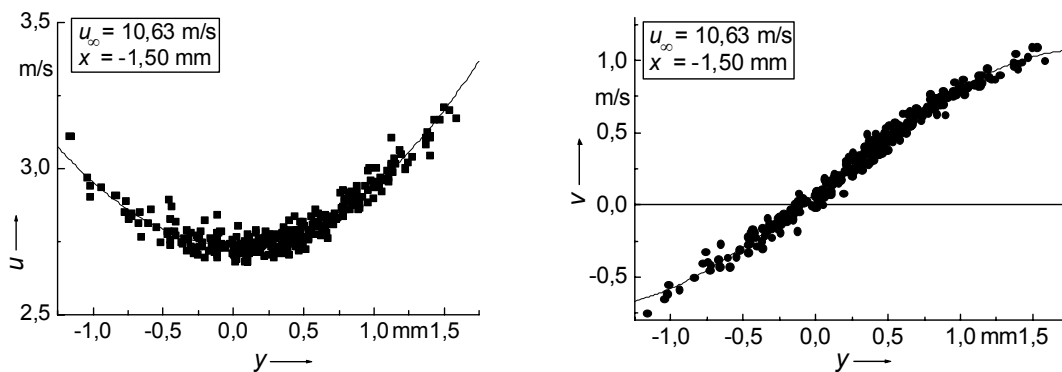


Fig. 6a,b Main stream and transverse component of flow in the vicinity of the stagnation point (6) of a cuboid

Velocity gradients are easily resolved. The effective length of the measuring volume now is only about 2,5 millimetres. Set-backs mainly arise from signal quality but also due to the finite span of the observation time window, the dynamic of velocity and non-planar flow. A standard acquisition system would have measured only one velocity. Because the spanwise velocity v is a function of the difference of both components of the two measuring volumes with a increasing separation away from the cross-over point, a severe problem exists for multi-component systems, when a gradient in the streamwise direction x is present as in case of the flow above. This is shown in figure 7, where the velocities v of all 11 positions have been plotted:

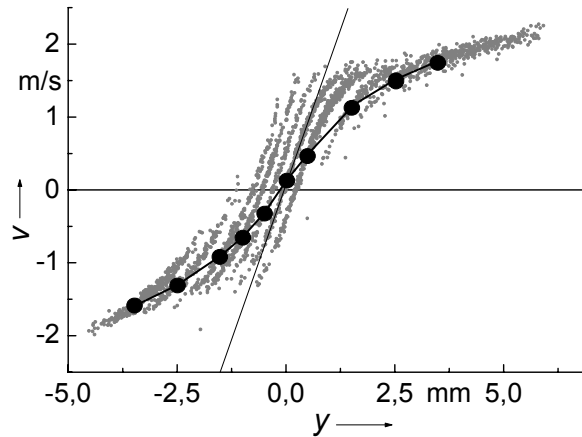


Fig. 7 Influence of gradient $\partial u/\partial x$ on the transverse velocity v at different positions

However, at the positions of the cross-over points (black dots in figure 7), the measurement is correct. Users of 2-D or 3-D systems should make their coincidence windows as small as possible. In our set-up we can assume a plane flow like that of a boundary layer and use the equation of continuity to subtract the local gradient by paying attention to the distance between both measuring volumes at this location. If not, the gradient has to be calculated at each cross-over point using the difference between fit (black line connecting the black dots) and linear regression through the data near the cross-over point (line drawn at $y = 0$). Knowing the interpolated gradient $\partial u/\partial x$ along y , the data can be corrected as shown in figure 8b.

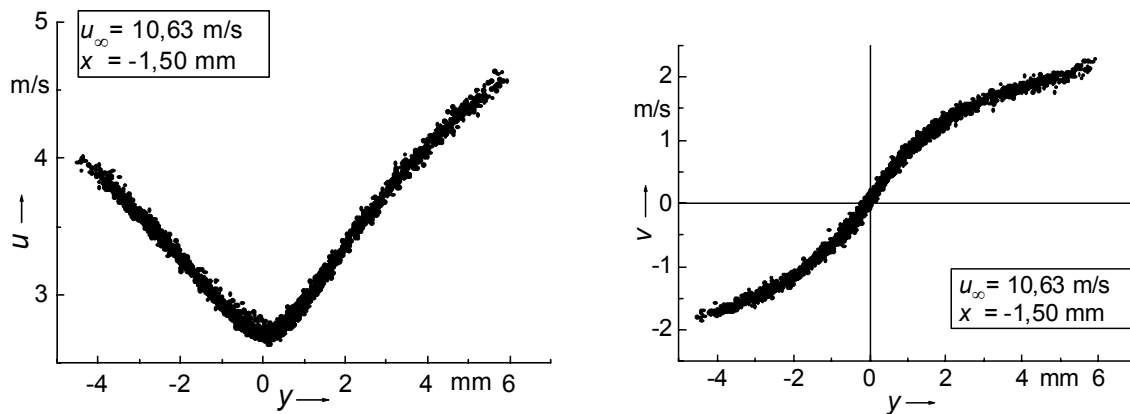


Fig. 8a,b Streamwise and transverse velocity near the stagnation point of a cuboid measured at 11 positions.

The influence of a streamwise gradient on the velocity u is not severe. If necessary, corrections can be done. At least, to measure a 3-D flows, data have to be taken from at least two different positions to account for gradients.

CONCLUSION

A time of flight evaluation of data from a commercially available 3D-LDA has been carried out. It shows the comfort to obtain small velocity profiles inside the measuring volumes without moving the probe. Manufacturers should provide the users with the arrival times of the LDA signals. This information is useful for the calibration of the fringe systems of the measuring volumes. It allows locally to define the fringe distance in order to reduce artificial turbulence. An increased spatial resolution due to time of flight data helps to acquire more precise data in areas where the flow changes rapidly. Streamwise gradients may corrupt the raw data, but their reduction is feasible.

At least in the overlapping region of three measuring volumes a spatially resolved 3D-velocity vector profiles can be obtained. In a plane flow the probe volume can be extended to some millimetres.

The method outlined exhibits the potential of a supposed data reduction of commercially available LDA-systems. The determination of “arrival times” and the path of a scattering particle through the probe has been shown in detail to help users to imitate the reduction shown above.

REFERENCES

Albrecht, H.-E.; Borys, M.; Hübner, K. (1993): Generalized theory for the simultaneous measurement of particle size and velocity using laser Doppler and laser two-focus methods. *Part. Part. Syst. Charact.* 10, pp. 138–145

Borys, M.; Strunck, V.; Müller, H.; Dopheide D. (2000): Simultaneous measurement of velocity and particle size profiles with the reference beam technique. 10th Int. Symp. on Applications of Laser Techniques to Fluid Mechanics, Lisbon, pp. 20.2.1–20.2.12

Strunck, V.; Grosche, G.; Dopheide, D. (1993): New laser Doppler sensors for spatial velocity information. Proc. Int. Congress on Instrumentation in Aerospace Simulation Facilities ICIASF'93, French-German Research Institute (ISL) Saint-Louis France, IEEE-Publ. 93CH3199-7, pp. 36.1–36.5

Strunck, V.; Grosche, G.; Dopheide, D. (1994): Scanning laser-Doppler probe for profile measurements. Proc. 7th Int. Symp. on Applications of Laser Techniques to Fluid Mechanics, Lisbon, pp. 17.1.1–17.1.5